BioNanoScience (2018) 8:835–844
https://doi.org/10.1007/s12668-018-0548-x

Green Synthesis of Silver Nanoparticles (AgNPs) from *Lenzites betulina* and the Potential Synergistic Effect of AgNP and Capping Biomolecules in Enhancing Antioxidant Activity

Marion Ryan C. Sytu[1] · Drexel H. Camacho[1,2]

Published online: 2 August 2018

Abstract
Properties of silver nanoparticles (AgNPs) are influenced by interactions and molecular structure of capping agents that stabilize them. Green synthesis of AgNPs using *Lenzites betulina*, a macrofungus with antioxidant properties, should be possible allowing the active metabolites or biomolecules to be incorporated in AgNP as capping molecules. Using surface plasmon resonance (SPR), the synthesis of AgNP using the aqueous extract of *L. betulina* was optimized. The purified *L.betulina*-capped AgNPs were then characterized and its antioxidant activity was compared with the raw *L. betulina* extract. The *L. betulina*-capped AgNPs exhibited SPR peak characteristic of AgNPs. Morphological analyses showed non-uniform spherical AgNP with visible intertwining capping agents engulfing the nanomaterial. FT-IR spectra revealed amide, carboxylate, and hydroxyl absorptions, confirming the role of some organic compounds as capping molecules. Extraction and complexation of the capping agent with SDS showed characteristic electronic excitation of phenylalanine along with tryptophan and tyrosine residues, suggesting the proteinaceous or polypeptide nature of the capping agent. The *L. betulina*-capped AgNPs were relatively stable (zeta potential − 26.7 mV), and the antioxidant activity was significantly enhanced compared to the raw extract. This is the first demonstration of *L. betulina* mushrooms in synthesizing AgNPs, the investigation of the proteinaceous capping biomolecules, and the enhanced effect of *L. betulina*-capped AgNPs in promoting stable radical reduction.

Keywords *Lenzites betulina* · Mushroom · Macrofungus · Silver nanoparticles · Green synthesis · Antioxidant

1 Introduction

Metal nanoparticles have unique optical, electronic, mechanical, magnetic, and chemical properties as compared to their bulk counterparts. These properties were attributed to their small size, which is in the range of 1 and 100 nm and to their extremely large surface area-to-volume ratio. For this reason, nanoparticles have been found to be useful in many applications like microelectronics, optical devices, catalysis, sensing, pharmaceuticals, and drug delivery [1]. Nanoparticles possess optical properties as they are small enough to confine their electrons and produce quantum effects. Surface plasmon resonance (SPR), an optical property of nanoparticles, is caused by the collective oscillations of the conduction electrons of nanoparticles upon irradiation with visible light. This gives the nanoparticle colloidal solution a characteristic color depending on the size and shape [1]. Among the metallic nanoparticles, silver has been very promising because it is an effective antimicrobial agent and good disinfectant with no adverse side effects, low toxicity in humans, and has diverse in vitro and in vivo applications [2]. Silver nanoparticles (AgNPs) are commonly synthesized chemically using a metal salt solution aided by reducing agents such as sodium borohydride, citrate, and ascorbic acid. Most etal nanoparticles are

Highlights
- Active metabolite separation through the process of silver nanoparticle (AgNP) synthesis
- Synergistic effect of the proteinaceous capping biomolecules from *L. betulina* mushroom and AgNPs
- Antioxidant activity of *L. betulina*-capped AgNPs enhances stable radical reduction

✉ Drexel H. Camacho
drexel.camacho@dlsu.edu.ph

Marion Ryan C. Sytu
marion.sytu@dlsu.edu.ph

[1] Chemistry Department, De La Salle University, 2401 Taft Avenue, 0922 Manila, Philippines

[2] Organic Materials and Interfaces Unit, CENSER, De La Salle University, 2401 Taft Avenue, 0922 Manila, Philippines

unstable due to aggregations, oxidations, etc. They are also intrinsically hydrophobic and easily tend to form aggregates in aqueous solution. These make nanoparticles lose their desirable properties. To prevent aggregations, stabilizers or capping molecules are incorporated in the synthesis of silver nanoparticles to ensure their stability in aqueous solutions. Some reducing agents also possess the added advantage of stabilizing the colloidal solution of the nanoparticles [3]. Capping molecules undergo interaction with AgNPs through electrostatic interaction, involving the coordination of anionic species that results in the formation of an electrical double layer, which causes coulombic repulsion and steric stabilization, where the presence of bulky materials impede the nanoparticles from diffusing together [4]. Multitudes of chemical reduction methods using inorganic and organic reducing agents have been utilized to synthesize stable and various shapes of silver nanoparticles usually in aqueous media [5]. Generally, specific control of shape, size, size distribution, and stability of AgNPs are often achieved by varying the synthesis methods, reducing agents, and stabilizers.

A green process in the synthesis of AgNPs offers a safe, benign, and eco-friendly alternative to the traditional protocols. Using aqueous extracts of natural products, silver nanoparticles can be synthesized without utilizing harmful reducing agents. Moreover, various natural products (carbohydrates, alkaloids, steroids, proteins, and/or peptides) in the aqueous extracts, capable of acting as both reducing and stabilizing agents, have been shown to efficiently synthesize nanoparticles. A cursory survey of the literature revealed very limited reports on the use of fungi in the preparation of nanometals [6]. Mushrooms are fungi that possess anti-inflammatory, cardiovascular, antitumor, and antibacterial properties in biological systems [7]. The bioactivities of mushrooms are attributed to the unique metabolites they contain making them a potential agent for synthesizing silver nanoparticles. Mushrooms are rich in proteins (about 40–49%) and have high availability of the amino acids lysine, tryptophan, glutamic acid, and aspartic acid [7, 8]. Silver nanoparticles formed from mushrooms are stabilized by proteins where interactions between silver nanoparticles and proteins lead to AgNP stabilization and formation of nanoparticle biomolecular-capped structures [9]. These interactions occur through covalent bonds and electrostatic interactions [10]. Of particular interest is the mushroom *Lenzites betulina* where studies on its metabolite contents showed the presence of benzoquinones and sterols [11, 12], which exhibited promising antibacterial and antioxidant activities [13]. In this study, *L. betulina* was explored for the first time for the synthesis of silver nanoparticles. The objectives of this study are to investigate *L. betulina* aqueous extract for the green synthesis of silver nanoparticles, to characterize the *L. betulina*-capped AgNPs and evaluate its antioxidant activity. Reported herein is the first demonstration of *L. betulina* mushrooms in synthesizing AgNPs, the investigation of the proteinaceous capping biomolecules in AgNP, and the enhanced effect of *L. betulina*-capped AgNPs in promoting stable radical reduction.

2 Materials and Methods

Silver nitrate, methanol, ethanol, 1% SDS (sodium dodecyl sulfate) solution, 1,1-diphenyl-2-picrylhydrazyl (DPPH) were purchased from www.sigmaaldrich.com and used as received. The mushroom *Lenzites betulina* samples were collected from Palawan, the Philippines, following collection protocols. Its identity was confirmed by the National Museum of the Philippines, and a sample was logged at the Chemistry Department, De La Salle University.

2.1 Preparation of Aqueous Extract of *L. betulina*

The air-dried mushroom (10 g) was washed thoroughly with distilled water, cut into smaller pieces, and crushed using a blender. The mushroom sample was immersed and stirred overnight in 250 mL distilled water in a beaker. After filtering using filter paper, the pale yellow extract was stored under refrigeration and further used for silver nanoparticle synthesis.

2.2 Optimization of Synthesis of Silver Nanoparticles

The method for synthesizing silver nanoparticles was optimized by varying the time and temperature parameters. Mushroom aqueous extract (10 mL) was mixed with 20 mL 1 mM aqueous $AgNO_3$. The synthesis was carried out in static condition under different temperature (RT, 60 and 90 °C) and time (1–7 h). Using UV-Vis spectrophotometry, the absorbance spectrum of each solution was obtained at 1-h intervals. The AgNPs from the optimized synthesis method was used for characterization and antioxidant assay.

2.3 Purification of Silver Nanoparticles

The colloidal solution of silver nanoparticles (as prepared) was purified by centrifugation (10,000 rpm for 15 min) using Sorvall® Super T21 Centrifuge. The supernatant, which contains the extract, excess silver, and nitrate ions, was discarded. The remaining silver nanoparticles were resuspended in distilled water and centrifuged. To ensure that the silver nanoparticles were completely devoid of any unbound organic molecules (from the mushroom extract), the resuspension and centrifugation were repeated thrice. The silver nanoparticle residues were then dried by lyophilization.

2.4 Characterization of Silver Nanoparticles

2.4.1 UV-Visible Spectrophotometry

UV-Visible spectrophotometry analysis (Hitachi U-2900) of the AgNPs was scanned at 300 to 700 nm. The presence of AgNPs (as synthesized) in the solution of *L. betulina* aqueous extract and $AgNO_3$ was confirmed by an absorbance peak at its surface plasmon resonance (~ 420 nm).

2.4.2 Field Emission Scanning Electron Microscopy/Energy-Dispersive X-Ray Spectroscopy

FESEM (FEI Helios NanoLab™ DualBeam™ 600i), in backscatter mode, was done on freeze-dried AgNPs mounted on the SEM holder. EDS analysis was carried out using an Oxford analyzer.

2.4.3 Transmission Electron Microscopy

TEM analysis (JEOL JEM-1220) was done on freeze-dried AgNPs, redispersed in distilled water under sonication, and placed on a carbon-coated copper grid. Samples were allowed to dry by evaporation at ambient temperature.

2.4.4 DLS and Zeta Potential

Dynamic light scattering (DLS) and zeta potential analysis (Malvern Zetasizer Nano ZS90) was done on freeze-dried AgNPs redispersed in distilled water under sonication and recorded three times.

2.4.5 XRD Analysis

X-ray diffraction (XRD) analysis was carried out on freeze-dried AgNPs using the Shimadzu Maxima XRD 7000 with a Ni-filtered CuK radiation source (k = 1.54 Â). The diffraction intensities were measured from 2θ = 0° to 55°.

2.4.6 FT-IR Spectroscopy

Fourier-transform infrared (FT-IR) analysis (Nicolet 6700) was carried out on freeze-dried *L. betulina* aqueous extract and the synthesized AgNPs. Samples were prepared in KBr powder (1:10).

2.5 Antioxidant Activity (DPPH Radical Scavenging Activity)

DPPH Radical Scavenging Assay method was done according to procedures reported by Abdel-Aziz et al. [14] with slight modifications. Freeze-dried *L. betulina* aqueous extract was dissolved in distilled water at a concentration of 0.2 mg/mL. Different volumes (200, 400, 600, 800, and 1000 μL) of the sample were measured in separate vials, and 2 mL of freshly prepared methanolic DPPH (0.2 mM) was added on each vial. The solutions were vortexed thoroughly and incubated in the dark for 30 min. The same process was done on freeze-dried AgNP dispersed in distilled water. The absorbance of each solution was recorded at around 517 nm. A DPPH solution (2 mL) was also kept in the dark for 30 min that served as the blank. The absorbance of each solution was obtained at 517 nm using UV-Vis spectrophotometry. The ability to scavenge DPPH radical was calculated using the equation:

$$\%\text{DPPH scavenging effect} = \left[\left(A_{\text{blank}} - A_{\text{sample}}\right)/A_{\text{blank}}\right] \times 100\%.$$

where

A_{blank} absorbance of 0.2 mM DPPH
A_{sample} absorbance of samples after 30 min of incubation

3 Results and Discussion

3.1 Synthesis of Silver Nanoparticles (AgNPs)

The formation of silver nanoparticles (AgNPs) from silver ions in the presence of reducing agents was monitored using UV-Vis spectrophotometry because AgNPs exhibit surface plasmon resonance (SPR), at around 420 nm. Generally, metal nanoparticles, because of their nano dimension, exhibit SPR phenomenon, where the metal electrons in the conduction band oscillate collectively in resonance at a certain wavelength of incident light. An aqueous extract of *Lenzites betulina* (Fig. 1a, b) in the presence of $AgNO_3$ at room temperature condition changed color from light yellow (Fig. 1c) to dark brown (Fig. 1d) solution after 2 days, suggestive of the formation of AgNPs. Verification through UV-Vis spectrophotometry (Fig. 1e) showed that a peak at 418 nm was observed, confirming the formation of AgNP at room temperature (RT) incubation for 2 days. In the absence of $AgNO_3$, the *L. betulina* aqueous extract solution did not undergo color change and no UV-Vis absorption was observed.

Inducing heat at 60 °C (Fig. 1f) during synthesis increases the absorbance at a shorter time indicating the accelerated formation of AgNPs. Increasing the temperature provides heat energy that increases the rate of reaction. As the reaction time increases, there is an apparent gradual increase in AgNP size as indicated by the red shift in λ_{max} (419 nm (1 h) to 434 nm (6 h)). The synthesis of nanoparticles and the reduction in size is strongly dependent on the availability of reducing agents and capping agents in the extract. The availability of the capping agents decreases as reaction time increases, resulting in the formation of bigger aggregated AgNPs since there are

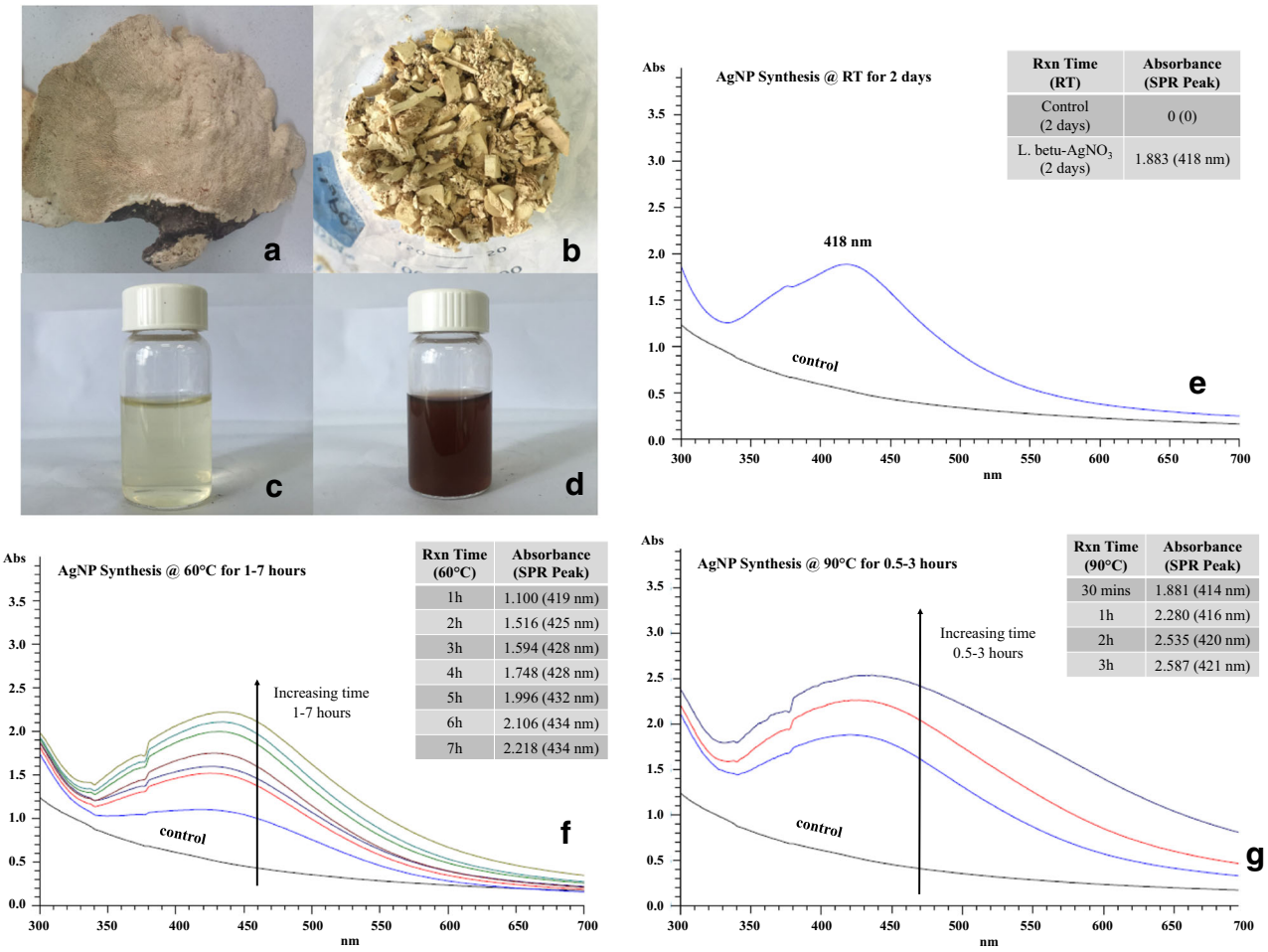

Fig. 1 **a** Air-dried *Lenzites betulina*. **b** Crushed *L. betulina*. **c** *L. betulina* aqueous solution. **d** *Lenzites betulina*-AgNP solution. UV-Vis spectra of *L. betulina*-AgNP solution **e** at RT, **f** at 60 °C, and **g** at 90°C (inset: absorbance and SPR data)

insufficient amounts of the capping agents available. Indeed, beyond 7 h of heating at 60 °C, the precipitate formation was observed. A higher synthesis temperature of 90 °C (Fig. 1g) further accelerated the formation of AgNPs where SPR absorbance reached 2.535 within 2 h of reaction time. The increase in reaction temperature showed the SPR peak shifting to lower wavelength region, indicating the formation of smaller nanoparticles. Increasing the reaction temperature caused a rapid reduction rate of the silver ions and the subsequent homogeneous nucleation of silver nuclei, which allows the formation of AgNPs with relatively smaller size [15]. The synthesis of silver nanoparticles carried out at 90 °C and 2 h gave the highest absorbance (highest AgNP yield) and shortest SPR peak (relatively smallest AgNP size) in a shorter amount of time and was considered as the optimized method. The AgNPs obtained using the optimized method was then purified for characterization and activity testing and were referred to hereon as *L. betulina*-capped AgNPs.

Lenzites sp. contains various metabolites that can potentially reduce Ag ions such as phenols, steroids, flavonoids, tannins, steroids, and saponins including sugars [16]. Sugars are efficient reducing agents for AgNP synthesis. In a study by Merca and Quizon [17], 180 kD lectins, which are glycoproteins, were isolated from *Lenzites* sp. The lectin was identified to contain 0.30% total sugars such as glucose, galactose, and maltose. The efficient reduction of Ag^+ ions using *L. betulina* aqueous extract can be attributed to the sugars in lectin, and since lectin is a protein, it can serve as the stabilizing agent because proteins are known to cap AgNPs.

3.2 Characterization of *L. betulina*-Capped AgNPs

3.2.1 Functional Group Analysis

The functional groups of the capping molecules stabilizing the *L. betulina*-capped AgNPs were analyzed by FT-IR (Fig. 2).

The *L. betulina* raw aqueous extract (Fig. 2a) shows peak at 3416 cm^{-1} representing the –OH stretch; 2925 cm^{-1} for C–H stretch; 1646 cm^{-1} for –C=O stretch; 1549 cm^{-1} for –N–H bend; 1380 cm^{-1} for C–O stretch and 1077 cm^{-1} for C–N

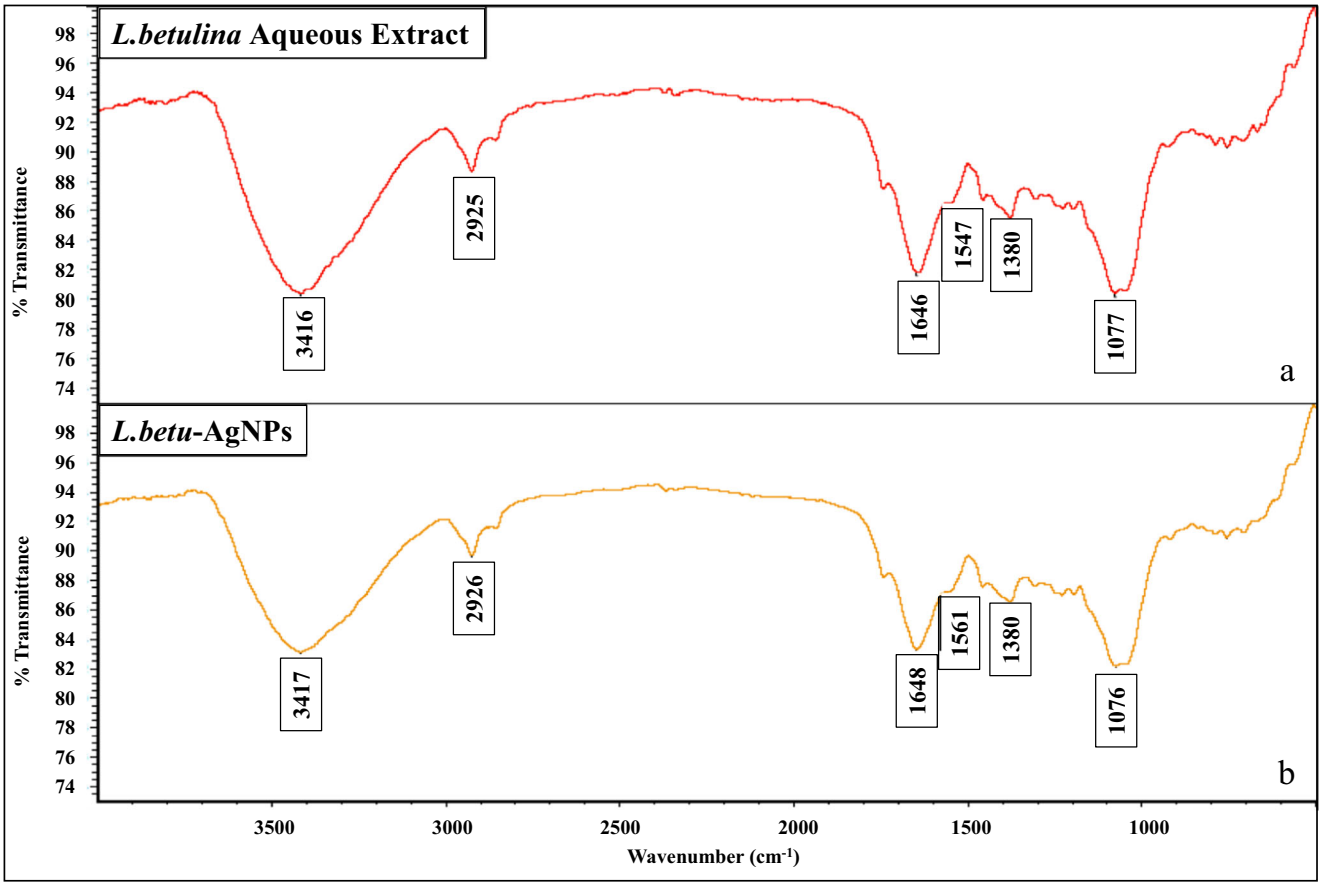

Fig. 2 FT-IR spectra of **a** *L. betulina* aqueous extract and **b** *L. betulina*-capped AgNPs

stretch. FT-IR spectra of *L. betulina*-capped AgNPs (Fig. 2b) showed similar IR absorption with the raw aqueous extract. Minor shifts, however, were observed for –OH stretching vibrations from 3416 to 3417 cm^{-1}; –C=O stretching from 1646 to 1648 cm^{-1}; –N–H bending from 1549 to 1561 cm^{-1} and C–N stretching from 1077 to 1076 cm^{-1}. The minor shifts in their stretching frequencies are attributed to the interaction of the capping molecules from *L. betulina* with the AgNPs. This confirms the role of some organic compounds (metabolites) in *L. betulina* as capping molecules for AgNPs. Characteristic bands usually found in the infrared spectra of proteins and polypeptides were observed such as the Amide I (stretching vibrations of the C=O bond of the amide) observed at 1648 cm^{-1} and Amide II (bending vibrations of the N–H bond of the amide) observed at 1561 cm^{-1} [18]. This indicates that upon reaction of *L. betulina* aqueous extract with silver nitrate, functional groups such as carboxyl, hydroxyl, and amide groups of the proteinaceous capping molecules may have participated in the reduction and stabilization process of silver nanoparticles. Also, the similar positions of the functional group bands of *L. betulina* aqueous extract and *L. betulina*-capped AgNPs indicate that the primary structure of the proteinaceous capping molecules is not affected as a consequence of reaction with the Ag^{+} ions or binding with the AgNPs [19]. It is known that protein-silver nanoparticle interactions can occur either through complex formation with free amine groups ($–NH_2$) or cysteine residues (–SH) in proteins and via the electrostatic attraction of negatively charged carboxylate groups (COO^{-}) [20]. The FT-IR results suggest the role of COO^{-} and $–NH_2$ in capping the AgNPs via electrostatic attraction and complex formation, respectively, suggesting that these biological molecules facilitate the formation and stabilization of the silver nanoparticles in an aqueous medium [21].

The presence of proteins or polypeptides coating the AgNPs was also indicated by UV-Vis spectrophotometry. The capping molecules were removed following the procedure developed by Jain et al. [22] and UV-Vis analysis confirms a peak at 265 nm (Fig. 3), attributed to the electronic excitations of phenylalanine along with tryptophan and tyrosine residues in proteins. The broad band observed (260–300 nm) is expected because combinations of these amino acids are incorporated as part of a polypeptide. The UV λ_{max} for AgNP-protein complexes as reported

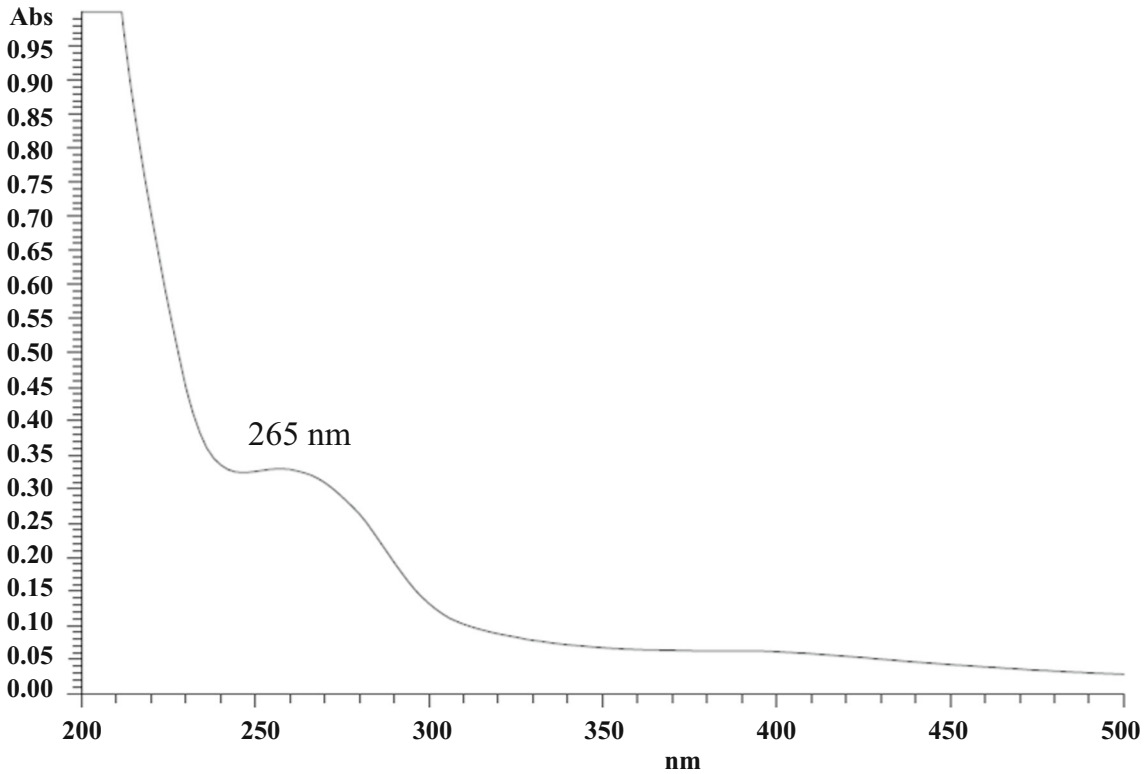

Fig. 3 Absorbance of SDS supernatant after SDS treatment of *L. betulina*-capped AgNPs

in the literature occurs at ~265 nm [1, 19, 23, 24] due to the favorable interaction between the nanoparticle and the protein through electrostatic interaction with free amine groups or cysteine residues in proteins [20]. The identity of the proteinaceous capping molecule is under investigation and will be reported elsewhere.

3.2.2 Elemental and Morphological Analysis

Elemental composition of the synthesized *L. betulina*-capped AgNPs showed an intense optical absorption band at 3.0 keV in EDS analysis, confirming the presence of pure metallic silver. Peaks for C, N, and O atoms were also observed (data are not shown), confirming nitrogenous or proteinaceous metabolites from *L. betulina* as capping molecules. XRD structural identification of *L. betulina*-capped AgNPs (Fig. 4) showed a broad diffraction peak at 38.22°, indicative of the presence of some amorphous regions. The diffraction peaks were indexed to [111] of face-centered cubic (fcc) silver [25]. Broader peaks for particles signify smaller particle and crystal size, allowing them to possess some amorphous regions compared to bulk materials [26]. Sharp diffraction peaks at 26.63°, 27.75°, 32.20°, and 46.20° were also observed, indicating high crystallinity. Dhoondia and Chakraborty [27] indexed the peaks at 27.75°, 32.20°, and 46.20° to [110], [111], and [211] of face-centered cubic (fcc) silver oxide, respectively, and is attributed to the fact that small AgNPs readily react with oxygen forming Ag_2O upon exposure to air [28]. However, Kumar et al. [29] suggested that

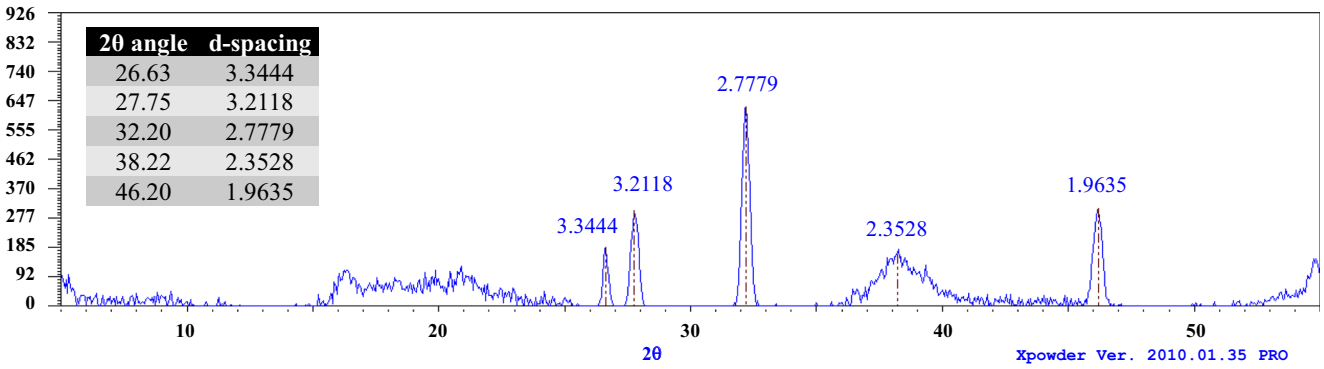

Fig. 4 X-ray diffraction pattern of *L. betulina*-capped AgNPs

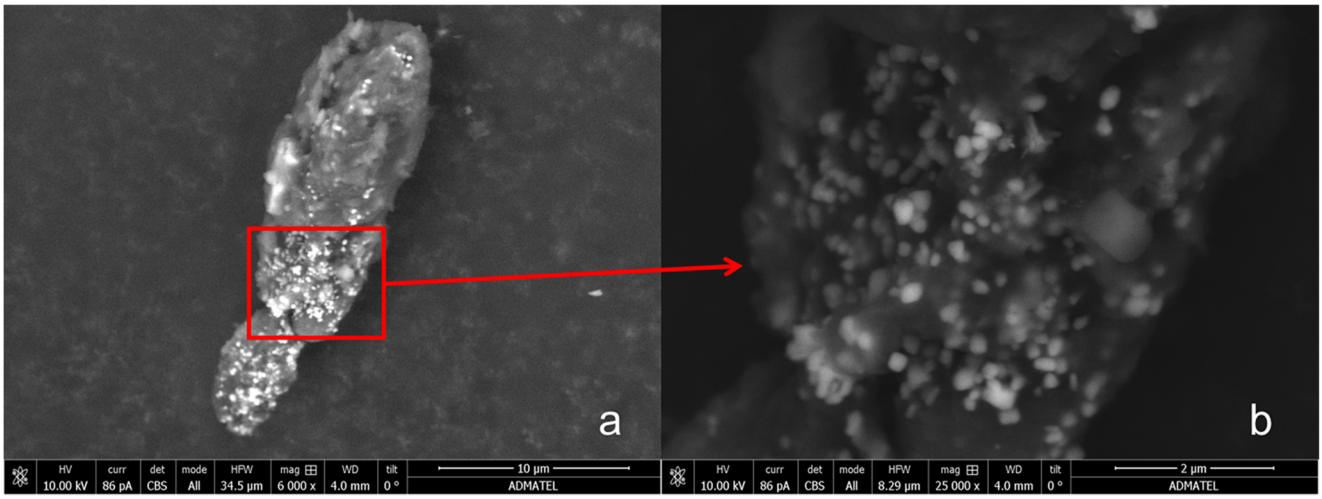

Fig. 5 SEM images (backscattered) of *L. betulina*-capped AgNPs magnified at **a** 6000× (scale bar 10 μm) and **b** 25,000× (scale bar 2 μm)

these three diffraction peaks are related to crystalline and amorphous organic structures accompanying the crystallized AgNPs.

FESEM images (Fig. 5) of *L. betulina*-capped AgNPs showed a lumped particle where spherical AgNPs are embedded in the lump. Backscatter mode confirms the presence of AgNP as they appear brighter. The AgNPs gave varying sizes ranging from 45 to 330 nm which is in agreement with a broad SPR peak at UV-Vis.

The shape, size, and size distribution of AgNPs are strongly dependent on the reducing power of organic substrates to reduce the silver ions [5]. The non-uniformity of the shapes and sizes of AgNPs from *L. betulina* is due to the heterogeneity of reducing agents in the extract. In contrast, AgNPs produced from chemical synthesis, which used a single reducing agent, have uniform morphologies [30]. TEM analysis (Fig. 6a) showed dispersed spherical silver nanoparticles. A closer look at some aggregates shows AgNPs in the size range of 14–50 nm. The capping molecules (gray) around the AgNP aggregates (Fig. 6b) are evident, which is reminiscent of a long-chain molecule or proteins entangled in the clusters of AgNPs.

The size distribution of *L. betulina*-capped AgNPs (Fig. 7) showed dispersed size range with an average hydrodynamic particle diameter of 270.8 nm. The DLS hydrodynamic diameter measures the diameter of the particle core, along with any capping molecules and a solvent layer attached to the particle. The same observation was observed by Ballotin et al. [9] on the hydrodynamic diameter of AgNP capped with proteins from fungus to have values at 264 nm as measured by DLS. The DLS average hydrodynamic diameter of *L. betulina*--capped AgNPs (270.8 nm) is way bigger than TEM measurement (14–50 nm), suggesting another evidence for the presence of a long-chain capping molecules entangled around AgNPs. The size distribution of nanoparticles shows two

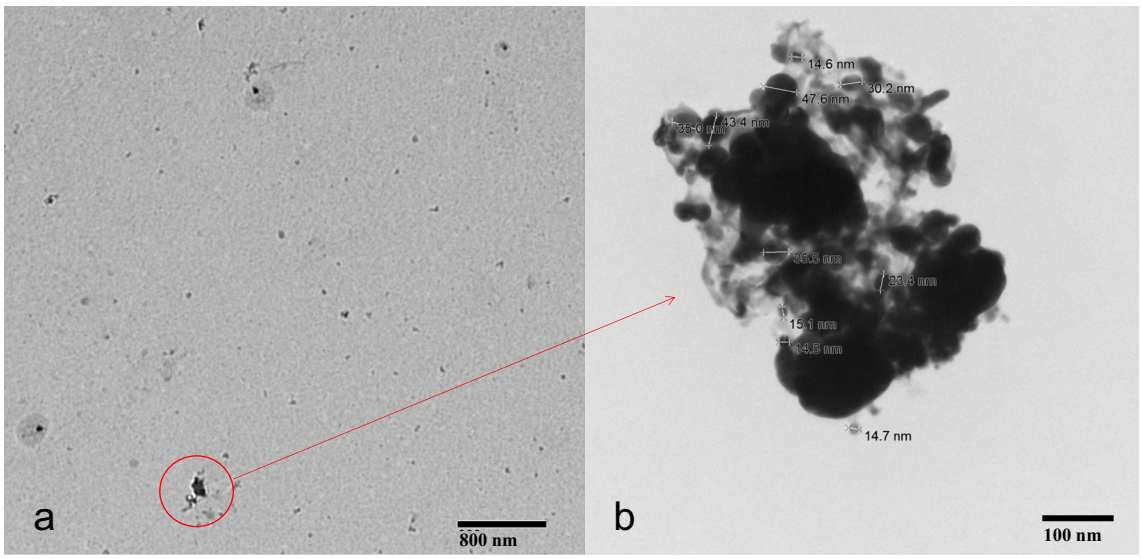

Fig. 6 TEM micrograph of *L. betulina*-capped AgNPs. **a** Dispersed AgNPs (23,500× magnification; 800 nm scale bar). **b** Aggregated AgNPs (156,000× magnification; 100 nm scale bar)

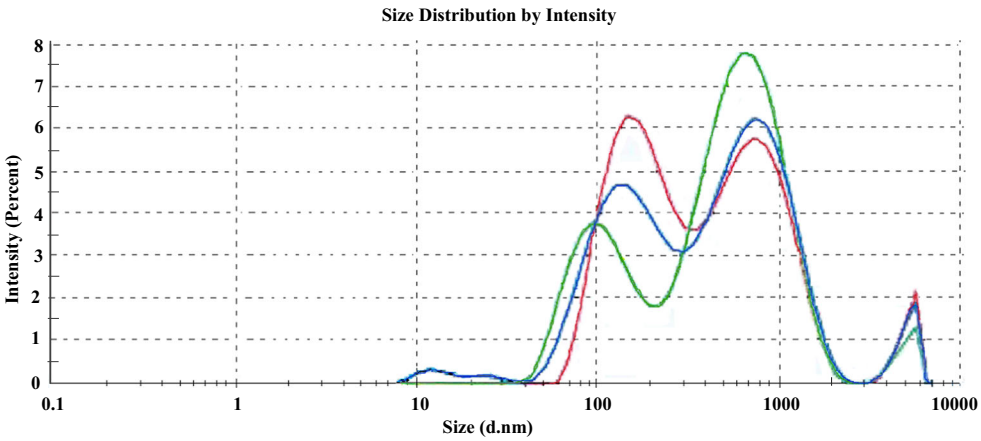

Fig. 7 Size distribution of *L.betulina*-capped AgNPs recorded three times

groups of peaks at around 95 to 400 and at 700 nm, which are likely the size range of different sets of AgNP aggregates. The formation of distinct bigger aggregates is likely attributed to the proteinaceous capping molecules around AgNPs, which could interact with other capping molecules forming a multilayer of nanosilver protein. Proteins are known to covalently bind to AgNPs and attract other proteins to form protein-protein specific or nonspecific interactions that become part of the nanosilver-protein multilayer [19]. The diverse size range is in agreement with the observed broad peak at SPR in UV-Vis spectrum of the *L. betulina*-capped AgNPs. The size distribution peak at greater than 1000 nm and less than 10,000 nm are due to the dust particles that might have contaminated the sample upon analysis.

Zeta potential of the *L. betulina*-capped AgNPs was measured at − 26.7 mV where incipient stability is at ≤ − 30 mV and at ≥ + 30 mV. The obtained zeta potenial indicates relative stability, supporting that AgNPs are likely to form aggregates with time. Previous studies showed that use of a strong reductant such as borohydride resulted in small particles that were monodispersed with a zeta potential of − 20 mV [31]. Using hydrazine hydrate as reducing agent produced AgNPs with a zeta potential of + 1.2 mV, while AgNPs from sodium citrate reduction possess a zeta potential of − 54 mV [31]. Synthesized AgNPs, using gallic acid as reducing and stabilizing agent, is extremely stable due to the strong electrostatic interaction of the carboxylate anion of the capping agent with the surface of the nanoparticle and a very high zeta potential at − 45 mV [32]. The relative stability of *L. betulina*-capped AgNPs is attributed to the long chain of proteinaceous capping agents unable to fully maximize the electrostatic interaction on all possible surfaces of AgNP because of chain coiling, entanglement, and protein-protein interactions which are in agreement with TEM, SEM, and DLS data.

3.3 Antioxidant Activity of *L. betulina*-Capped AgNPs

The DPPH radical scavenging assay of *L. betulina* aqueous extract and *L. betulina*-capped AgNPs showed that the raw aqueous extract (Table 1, column 3) possesses an inherent antioxidant activity. A slight increase in antioxidant activity of *L. betulina*-capped AgNPs (Table 1, column 4) was observed. The increase in antioxidant activity of *L. betulina*-capped AgNPs can be attributed to the higher surface area-to-volume ratio of silver nanoparticles, enhancing their reactivity towards DPPH. Statistical analysis using a paired *t* test, which compares the differences of %Inhibition values obtained from the two samples, showed that the two are significantly different. The $t_{calculated}$ value (17.45) is greater than t_{table} value for 99% confidence interval (4.604) with 4 degrees of freedom (n−1; $n = 5$).

Table 1 Mean antioxidant activities of *L. betulina* and *L. betulina*-capped AgNPs with their standard deviation values

Volume of samples (μL)	Final Concentration (μg/mL)	%Inhibition /antioxidant Activity	
		L. betulina aqueous extract	*L. betulina*-capped AgNPs
0	0	0	0
200	18.18	11.33 ± 0.35	13.46 ± 0.78
400	33.33	17.92 ± 0.29	19.75 ± 1.67
600	46.15	26.59 ± 0.50	28.90 ± 0.99
800	57.14	31.35 ± 0.60	33.01 ± 1.03
1000	66.67	37.77 ± 1.49	39.69 ± 1.01

This means that there is greater than a 99% chance that the results from the two samples are significantly different, indicating *L. betulina*-capped AgNPs have significantly higher antioxidant activity than *L. betulina* aqueous extract.

Biosynthesized AgNPs are effective antioxidants compared to chemically prepared AgNP due to their capping agents. Fungi, having different chemical constituents compared to plants, offer capping agents that provide synergistic activity with AgNP. Mathew et al. [33] reported the antioxidant activity of the protein-capped silver nanoparticles synthesized from the fungus *Aspergillus pseudodeflectus*, which gave a %inhibition of 17.59 ± 2.28 at a final concentration of 62.5 μg/mL. Notably, the activity of *L. betulina*-capped AgNPs was higher than that of AgNPs from the fungus *Aspergillus pseudodeflectus*. Proteins act as free radical scavengers, owing their antioxidant activity to their constituent amino acids [34]. Antioxidant activities of tyrosine, phenylalanine, and tryptophan are due to their ability to donate protons to free radicals whereas lysine, arginine, aspartic acid and glutamic acid, exercise antioxidant activity by chelating metal ions [35]. The enhanced antioxidant activity of *L. betulina*--capped AgNPs compared to the raw extract is interesting because antioxidants lay a chemo-protective key role in humans against risk of oxidative stress-related diseases [36]. *L. betulina* aqueous extract has been shown to possess antimicrobial, anti-cancer [13], and anti-hyperglycemic [37] activities and the presence of these active metabolites in AgNP may provide synergistic effects potentially enhancing the activities as demonstrated by this study. Moreover, using the simple protocol of AgNP synthesis, the study demonstrated the possibility of separating and isolating the active components in a plant or fungus source from the rest of the metabolites. This helps advance the field of possible selective metabolite extraction from biological sources and promote the fast screening of metabolites using this simple process of natural product isolation.

4 Conclusion

AgNPs were successfully and optimally synthesized using the aqueous extract of the fungus *L. betulina* for the first time. Characterization of the new *L. betulina*-capped AgNPs showed spherical shapes in varying size in nano dimension with likely proteinaceous capping molecules. The *L. betulina*-capped AgNPs were relatively stable due to the capping molecules but formed some aggregates with time. The DPPH assay showed that *L. betulina*-capped AgNPs exhibited significantly higher antioxidant activities compared to its raw aqueous extract. The properties of silver nanoparticles (AgNPs) were influenced by interactions and molecular structure of capping agents that stabilize them. Green synthesis of AgNPs using *Lenzites betulina*, a macrofungus with antioxidant properties, was made possible allowing the active metabolites to be incorporated in AgNP as capping molecules and enhancing significantly the antioxidant activity compared to the raw extract. Notably, the activity of *L. betulina*-capped AgNPs was remarkably higher than that of AgNPs from the fungus *Aspergillus pseudodeflectus*. Full characterization of the proteinaceous capping metabolite on the AgNP surface is underway and will be reported in due course.

Funding This work was supported by DLSU-URCO and National Research Council of the Philippines (NRCP)-DOST.

Compliance with Ethical Standards

Conflict of Interest The authors declare that they have no conflict of interest.

References

1. Basavaraja, S., Balaji, S. D., Lagashetty, A., Rajasab, A. H., & Venkataraman, A. (2008). Extracellular biosynthesis of silver nanoparticles using the fungus *Fusarium semitectum*. *Materials Research Bulletin, 43*, 1164–1170. https://doi.org/10.1016/j.materresbull.2007.06.020.
2. Dipankar, C., & Murugan, S. (2012). The green synthesis, characterization, and evaluation of the biological activities of silver nanoparticles synthesized from *Iresine herbstii* leaf aqueous extracts. *Colloids and Surfaces. B, Biointerfaces, 98*, 112–119. https://doi.org/10.1016/j.colsurfb.2012.04.006.
3. Cataldo, F., Ursini, O., & Angelini, G. (2013). A green synthesis of colloidal silver nanoparticles and their reaction with ozone. *Eur Chem Bull, 2*, 700–705. https://doi.org/10.17628/ecb.2013.2.700-705.
4. Abou El-Nour, K. M. M., Eftaiha, A., Al-Warthan, A., & Ammar, R. A. A. (2010). Synthesis and applications of silver nanoparticles. *Arabian Journal of Chemistry, 3*, 135–140. https://doi.org/10.1016/j.arabjc.2010.04.008.
5. Hussain, J., Kumar, S., Hashmi, A. A., & Khan, Z. (2011). Silver nanoparticles: preparation, characterization, and kinetics. *Adv Mat Lett, 2*, 188–194. https://doi.org/10.5185/amlett.2011.1206#sthash.kTIvbUae.dpuf.
6. Sudhakar, T., Nanda, A., Babu, S. G., Janani, S., Evans, M. D., & Markose, T. K. (2014). Synthesis of silver nanoparticles from edible mushroom and its antimicrobial activity against human pathogens. *Int J PharmTech Res, 6*, 1718–1723.
7. Philip, D. (2009). Biosynthesis of Au, Ag and Au-Ag nanoparticles using edible mushroom extract. *Spectrochimica Acta. Part A, Molecular and Biomolecular Spectroscopy, 73*, 374–381. https://doi.org/10.1016/j.saa.2009.02.037.
8. Hsu, T. H., Shiao, L. H., Hsieh, C., & Chang, D. M. (2002). A comparison of the chemical composition and bioactive ingredients of the Chinese medicinal mushroom DongChongXiaCao, its counterfeit and mimic, and fermented mycelium of *Cordyceps sinensis*. *Food Chemistry, 78*, 463–469. https://doi.org/10.1016/S0308-8146(02)00158-9.
9. Ballottin, D., Fulaz, S., Souza, M. L., Corio, P., Rodrigues, A. G., Souza, A. O., Gaspari, P. M., Gomes, A. F., Gozzo, F., & Tasic, L. (2016). Elucidating protein involvement in the stabilization of the biogenic silver nanoparticles. *Nanoscale Research Letters, 11*, 313. https://doi.org/10.1186/s11671-016-1538-y.

10. Chung, Y. C., Chen, I. H., & Chen, C. J. (2008). The surface modification of silver nanoparticles by phosphoryl disulfides for improved biocompatibility and intracellular uptake. *Biomaterials, 29*, 1807–1816. https://doi.org/10.1016/j.biomaterials.2007.12.032.
11. Lee, I. N., Yun, B. S., Cho, S. M., Kim, W. G., Kim, J. P., Ryoo, I. J., Koshino, H., & Yoo, I. D. (1996). Betulinans a and B, two benzoquinone compounds from *Lenzites betulina*. *Journal of Natural Products, 59*, 1090–1092. https://doi.org/10.1021/np960253z.
12. Liu, K., Wang, J. L., Wu, H. B., Wang, Q., Bi, K. L., & Song, Y. F. (2012). A new pyranone from *Lenzites betulina*. *Chem Nat Comp, 48*, 780–781. https://doi.org/10.1007/s10600-012-0380-4.
13. Liu, K., Wang, J. L., Zhao, L., & Wang, Q. (2014). Anticancer and antimicrobial activities and chemical composition of the birch Mazegill mushroom *Lenzites betulina* (higher basidiomycetes). *Int J Med Mushrooms, 16*, 327–337. https://doi.org/10.1615/IntJMedMushrooms.v16.i4.30.
14. Abdel-Aziz, M. S., Shaheen, M. S., El-Nekeety, A. A., & Abdel-Wahhab, M. A. (2014). Antioxidant and antibacterial activity of silver nanoparticles biosynthesized using *Chenopodium murale* leaf extract. *Journal of Saudi Chemical Society, 18*, 356–363. https://doi.org/10.1016/j.jscs.2013.09.011.
15. Khalil, M. M. H., Ismail, E. H., El-Baghdady, K. Z., & Mohamed, D. (2014). Green synthesis of silver nanoparticles using olive leaf extract and its antibacterial activity. *Arabian Journal of Chemistry, 7*, 1131–1139. https://doi.org/10.1016/j.arabjc.2013.04.007.
16. Fakoya, S., & Oloketuyi, S. F. (2012). Antimicrobial efficacy and phytochemical screening of mushrooms, *Lenzites betulinus*, and *Coriolopsis gallica* extracts. *TAF Prev Med Bull, 11*, 695–698. https://doi.org/10.5455/pmb.1-1327262044.
17. Merca, F. E., & Quizon, R. V. (2002). Isolation, purification and characterization of a lectin from *Lenzites* sp. *Philipp Agric Sci, 85*, 180–191.
18. Garidel, P., & Schott, H. (2006). Fourier-transform midinfrared spectroscopy for analysis and screening of liquid protein formulations. *Bioprocess International*, 48–55.
19. Ahmad, A., Mukherjee, P., Senapati, S., Mandal, D., Khan, M. I., Kumar, R., & Sastry, M. (2003). Extracellular biosynthesis of silver nanoparticles using the fungus *Fusarium oxysporum*. *Colloids and Surfaces. B, Biointerfaces, 28*, 313–318. https://doi.org/10.1016/S0927-7765(02)00174-1.
20. Selvi, V. K., & Sivakumar, T. (2012). Isolation and characterization of silver nanoparticles from *Fusarium oxysporum*. *International Journal of Current Microbiology and Applied Sciences, 1*, 56–62.
21. Quester, K., Avalos-Borja, M., & Castro-Longoria, E. (2016). Controllable biosynthesis of small silver nanoparticles using fungal extract. *J Biomater Nanobiotechnol, 7*, 118–125. https://doi.org/10.4236/jbnb.2016.72013.
22. Jain, N., Bhargava, A., Rathi, M., Dilip, R. V., & Panwar, J. (2015). Removal of protein capping enhances the antibacterial efficiency of biosynthesized silver nanoparticles. *PLoS One, 10*. https://doi.org/10.1371/journal.pone.0134337.
23. Durán, N., Marcato, P. D., Alves, O. L., De Souza, G. I. H., & Esposito, E. (2005). Mechanistic aspects of biosynthesis of silver nanoparticles by several *Fusarium oxysporum* strains. *Journal of Nanbiotechnology, 3*(8). https://doi.org/10.1186/1477-3155-3-8.
24. Phanjom, P., & Ahmed, G. (2015). Biosynthesis of silver nanoparticles by *Aspergillus oryzae* (MTCC no. 1846) and its characterizations. *Nanoscience and Nanotechnology, 5*, 14–21.
25. Shihab, R. N., Al-Kalifawi, E. J., & Al-Haidari, S. H. J. (2016). Environmental friendly synthesis of silver nanoparticles using leaf extract of Mureira tree (*Azadirachta indica*) cultivated in Iraq and efficacy the antimicrobial activity. *Journal of Natural Science Research, 6*, 47–56.
26. Umadevi, M., Shalini, S., & Bindhu, M. R. (2012). Synthesis of silver nanoparticles using *D. carota* extract. *Advances in Natural Sciences: Nanoscience and Nanotechnology, 3*(025008). https://doi.org/10.1088/2043-6262/3/2/025008.
27. Dhoondia, Z. H., & Chakraborty, H. (2012). *Lactobacillus* mediated synthesis of silver oxide nanoparticles. *Nanomater Nanotechno, 2*, 1–7. https://doi.org/10.5772/55741.
28. Xiao, F., Liu, H. G., & Lee, Y. I. (2008). Formation and characterization of two-dimensional arrays of silver oxide nanoparticles under Langmuir monolayers of n-hexadecyl dihydrogen phosphate. *Bulletin of the Korean Chemical Society, 29*, 2368–2372. https://doi.org/10.5012/bkcs.2008.29.12.2368.
29. Kumar, R., Roopan, S. M., Prabhakarn, A., Khanna, V. G., & Chakroborty, S. (2012). Agricultural waste *Annona squamosa* peel extract: biosynthesis of silver nanoparticles. *Spectrochimica Acta. Part A, Molecular and Biomolecular Spectroscopy, 90*, 173–176. https://doi.org/10.1016/j.saa.2012.01.029.
30. Mavani, K., & Shah, M. (2013). Synthesis of silver nanoparticles by using sodium borohydride as a reducing agent. *Int J Eng Res Tech, 2*(2), 1–5. https://doi.org/10.13140/2.1.3116.8648.
31. Sodha, K. H., Jadav, J. K., Gajera, H. P., & Rathod, K. J. (2015). Characterization of silver nanoparticles synthesized by different chemical reduction methods. *International Journal of Pharma and Bio Sciences, 6*, 199–208.
32. Yoosaf, K., Ipe, B. I., Suresh, C. H., & Thomas, K. G. (2007). In situ synthesis of metal nanoparticles and selective naked-eye detection of lead ions from aqueous media. *Journal of Physical Chemistry C, 111*, 12839–12847. https://doi.org/10.1021/jp073923q.
33. Mathew, J., Rathod, V., Singh, D., Singh, A. K., & Kulkarni, P. (2016). Antioxidant potential of AgNPs from the fungus *Aspergillus pseudodeflectus* by DPPH radical scavenging assay. *Int J Pharm Pharm Sci Res, 6*, 6–11.
34. Zieli ski, H., & Koz owska, H. (2000). Antioxidant activity and total phenolics in selected cereal grains and their different morphological fractions. *Journal of Agricultural and Food Chemistry, 48*, 2008–2016. https://doi.org/10.1021/jf990619o.
35. Ramakrishna, H., Murthy, S. S., Divya, R., MamathaRani, D. R., & Pandarunga, M. G. (2012). Hydroxy radical and DPPH scavenging activity of crude protein extract of *Leucas linifolia*: a folk medicinal plant. *Asian J Plant Sci Res, 2*, 30–35.
36. Ranjitham, A. M., Suja, R., Caroling, G., & Tiwari, S. (2013). In vitro evaluation of antioxidant, antimicrobial, anticancer activities and characterization of *Brassica oleracea*. var. Bortrytis. L synthesized silver nanoparticles. *International Journal of Pharmacy and Pharmaceutical Sciences, 5*, 239–251.
37. Hussin, F. R. M., Vitor, I. I. R. J. S., Joaquin, J. A. O., Clerigo, M. M., & Paano, A. M. C. (2016). Anti-hyperglycemic effects of aqueous *Lenzites betulina* extracts from the Philippines on the blood glucose levels of the ICR mice (*Mus musculus*). *Asian Pac J Trop Biomed, 6*, 155–158. https://doi.org/10.1016/j.apjtb.2015.04.013.